Quantum melting and lattice orientation of driven vortex matter

S. Okuma, H. Imaizumi, and D. Shimamoto
Research Center for Low Temperature Physics, Tokyo Institute of Technology, 2-12-1, Ohokayama, Meguro-ku, Tokyo 152-8551, Japan

N. Kokubo
Center for Research and Advancement in Higher Education, Kyushu University, 4-2-1, Ropponmatsu, Chuoh-ku, Fukuoka 810-0044, Japan
(Received 31 August 2010; revised manuscript received 30 December 2010; published 28 February 2011)

We investigate the lattice orientation of driven vortex matter prior to dynamic melting at the field $B_{c,\mathrm{dyn}}$ (i.e., melting for driven vortex lattices) in an amorphous Mo_xGe_{1-x} film using a mode-locking technique. Under increasing field B at fixed temperatures T, we observe a switching of the lattice orientation from a perpendicular to parallel orientation at a T-dependent characteristic field $B_{\mathrm{ori}}(T)$. The shape of the $B_{\mathrm{ori}}(T)$ line in the B-T plane resembles that of the dynamic melting line $B_{c,\mathrm{dyn}}(T)$, $B_{\mathrm{ori}}(T) \approx 0.8B_{c,\mathrm{dyn}}(T)$, while $B_{c,\mathrm{dyn}}(T)$ at low T is significantly suppressed compared to a static melting line due to quantum effects. The results reveal that the lattice rotation occurs as a precursor of dynamic melting instead of static melting and it possibly arises from reduced effective pinning prior to dynamic melting.

DOI: 10.1103/PhysRevB.83.064520 PACS number(s): 74.25.Uv, 74.25.Dw, 74.25.Ha

I. INTRODUCTION

The motion of periodic media driven over pinning potentials, which appears widely in nature, has been studied extensively over the years in many systems.[1–3] The vortices in type-II superconductors have been used as a general model system to study such a phenomenon[4] as well as various nonequilibrium many-body effects.[5–7] This is because the vortices form an ordered lattice by vortex-vortex interactions, the strength of which can be varied over a broad range by simply changing the magnetic field B, and its dynamics is readily controlled by the Lorentz force due to the applied current I. In the presence of random pinning originating from material defects, several dynamic phases of driven vortices with different temporal, positional, and orientational orders are realized depending on the amplitude of driving forces or velocities v. At small v, the vortex motion is described as pinning-induced disordered flow, such as, plastic and smectic flows.[8–11] With increasing v, the influence of the pinning potential becomes effectively reduced and the pinning-dominated incoherent flow changes to interaction-dominated coherent flow, where the vortices crystallize into a moving lattice.[1,12–16] The moving lattice has limited degree of freedom in orientation and it may be characterized by the lattice vector parallel to the flow direction.[16] On approaching the mean-field line $B_{c2}(T)$ by increasing magnetic field(B)/temperature(T), the lattice order in moving vortices becomes unstable against thermal fluctuations, and the moving vortex lattice would melt into a liquid-like moving state. This is called "dynamic" melting, which may occur near the "static" melting point of vortex lattice into vortex liquid.

When strong quantum fluctuations are present, an interesting possibility would appear in the moving vortex states: The moving vortex lattice may melt into a quantum moving liquid from the analogy to the quantum melting of the vortex lattice into a quantum vortex liquid.[17–19] Several experimental studies reported on the presence of the quantum vortex-liquid regime at low temperatures close to $T = 0$ and high fields close to the second critical field B_{c2}.[18,20–23] However, experimental evidence for quantum melting of the vortex lattice has not yet been obtained. This is partly related to the fact that in the relevant temperature and field range, the influences of the quenched disorder (random pinning) upon vortices are strong and they give rise to a structural transition from an ordered vortex lattice state into a disordered amorphouslike vortex state,[24–27] accompanied by a peak in the critical current I_c known as a peak effect (PE).[28–34] Thus, the experimental studies reported so far would merely deal with a (gradual) transition from the amorphous vortex state to the quantum vortex liquid state, which is not an "intrinsic" quantum melting phenomenon of vortex lattice.

This difficulty may be overcome by simply driving vortices by the transport current since the influences of the quenched disorder can be effectively reduced at large vortex velocity. A recent mode-locking (ML) experiment in amorphous superconductors would shed light on this issue.[35] The ML is the dynamic resonance between the rf current superimposed on the dc current and the periodic motion of driven vortex lattice, and it probes sensitively the lattice order in driven vortices.[1,36–43] On approaching the mean-field line $B_{c2}(T)$ by increasing magnetic field, the resonant feature becomes smeared due to the disruption of the shear rigidity in driven vortex lattice by thermal and/or quantum fluctuations and it sharply disappears at the dynamic melting point $B_{c,\mathrm{dyn}}$. The obtained dynamic melting line $B_{c,\mathrm{dyn}}(T)$ shows a unique temperature dependence at low temperatures: The temperature dependence of $B_{c,\mathrm{dyn}}(T)$ is much weaker than the mean-field line $B_{c2}(T)$. This indicates the wide opening of the moving liquid region at the limit of $T = 0$, suggesting the influence of strong quantum fluctuations expected in high (normal-state) resistivity films of amorphous superconductors.

Another important feature with the ML resonance is that one can probe the orientation of driven vortex lattice with respect to the flow direction.[44] A theoretical argument based on an idea of the least power dissipation showed that at large velocities the motion of vortices driven over random pinning potential is parallel to their nearest-neighbor direction (i.e., parallel orientation),[16] as schematically illustrated in Fig. 1(a). This is consistent with the experimental result on Al granular films in Ref. 36. By contrast, a recent ML study on amorphous

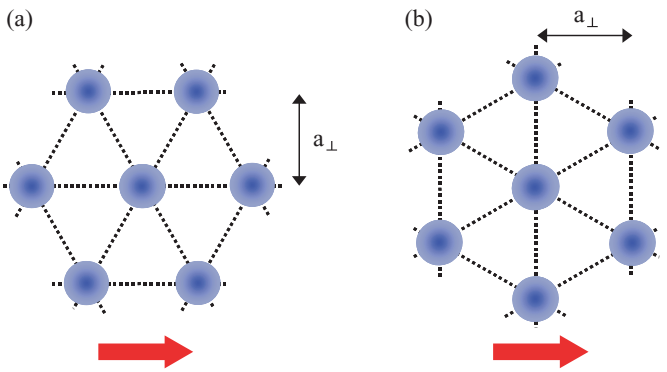

FIG. 1. (Color online) (a) Schematic illustration of vortex lattices moving with parallel and (b) perpendicular orientations with respect to the flow directions. The flow directions and the row spacing $a_\perp$ are indicated with thick and thin arrows, respectively.

films conducted at relatively high temperatures[44] has shown compelling evidence for the perpendicular orientation of driven vortex lattice [Fig. 1(b)]. Moreover, on approaching the mean-field line the moving lattice rotates from the perpendicular to parallel orientations and it occurs near (but prior to) the dynamic melting point. This may imply that the lattice orientation is relevant to the lattice softening due to the thermal fluctuations, although the mechanism behind the phenomenon remains unresolved.

The phenomenon of lattice rotation would be interesting when the quantum fluctuations are relevant. In this study, we present detailed measurements of the ML resonance over the broad field range including the high-field region near the dynamic melting point at different temperatures down to 0.8 K, where quantum melting of driven lattices may occur. We find that the rotation of the lattice orientation occurs as a precursor for dynamic melting and it does not have direct relationship with equilibrium vortex states. A possible interpretation of the data based on recent simulation work[45] will be discussed.

II. EXPERIMENTAL

The 330-nm-thick a-Mo_xGe_{1-x} film was fabricated by rf sputtering onto a silicon substrate mounted on a water-cooled rotating copper stage.[46] The mean-field transition temperatures T_{c0} defined by a 95% criterion of the normal-state dc linear resistivity,[23] $\rho(T_{c0}) = 0.95\rho_n$, and the zero-resistivity temperatures T_c are 6.1 and 6.0 K, respectively. The resistivity ρ and I-V characteristics were measured using a standard four-terminal method. In measuring the ML resonance, the ac current I_{rf} with a frequency f_{ext} of up to 10 MHz was applied through an rf transformer.[35,47] Here, we used a function generator (NF Wave-Factory), which enables us to apply the ac current I_{rf} superimposed with the dc current I without using a dc current source, and a nanovolt meter (HP 34420A) for measuring V. Batteries are also used instead of the function generator as a dc current source for measurements with reduced noise. The film was attached to the cold plate of our ^{3}He-^{4}He dilution refrigerator. We also immersed the film directly into liquid ^{4}He for the measurements at 4 K. The field was applied perpendicular to the plane of the film.

All the data presented in this paper were measured in zero-field-cooled mode. To examine a possible history dependence, some I-V data including those in the PE regime were also taken in field-cooled mode, namely, the field was applied in the normal state and then the film was cooled through T_c with no applied current. However, a significant difference between the two modes is not observed for all the data examined, in contrast to the behavior reported in $NbSe_2$ single crystals.[24]

III. RESULTS AND DISCUSSION

First, let us outline the equilibrium vortex states in the a-Mo_xGe_{1-x} film that are relevant to the interpretation of the data of ML. From the I-V characteristics, we define the critical (depinning) current I_c as a threshold current at which the vortices start to move, where a 10^{-7} V criterion is used.[47,48] The peak in the $I_c(B)$ curve indicative of PE[28–34] is visible over the whole temperature region (T = 0.08–5.0 K). The representative data are shown in Fig. 2(a). Combined with

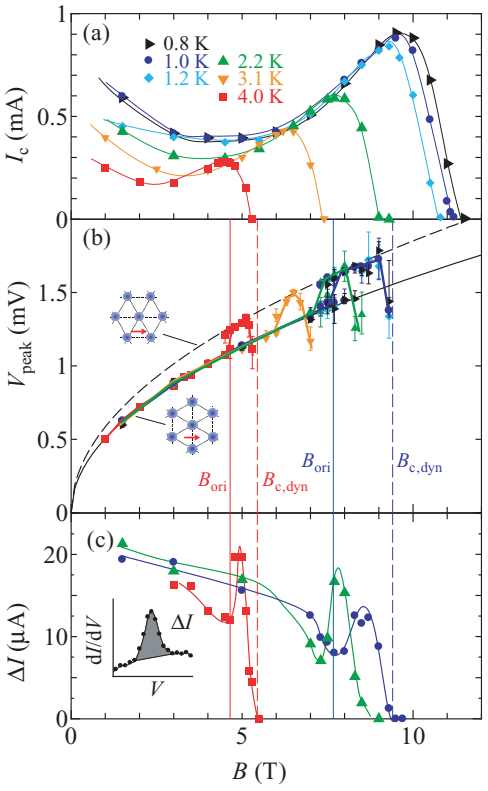

FIG. 2. (Color online) (a) The B dependence of I_c at different temperatures, which are listed in the figure. (b) V_{peak} vs B measured at different temperatures. Solid and dashed curves represent $V_{1/2}^{perp}(B)$ and $V_{1/1}^{para}(B)$, respectively. (Insets) Schematic diagrams of moving vortex lattices, where arrows indicate the directions of the vortex motion. (c) ML step width ΔI vs B at selected T. Symbols in (b) and (c) correspond to those in (a). In (b) and (c), vertical solid and dashed lines indicate B_{ori} and $B_{c,dyn}$, respectively; left (red) and right (blue) lines correspond to the fields at 4.0 and 1.0 K, respectively. Other lines are guides for the eye. The width of the ML current step is obtained by integrating the peak of the dI/dV vs V curves with respect to the flux-flow baseline, as schematically illustrated in the inset of (c).

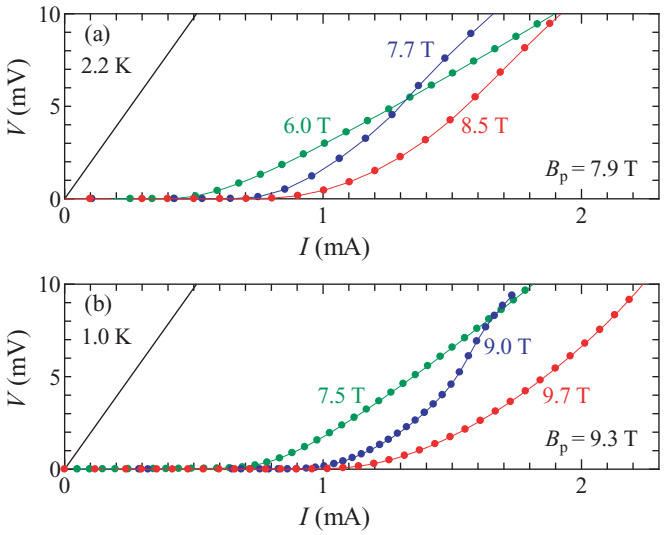

FIG. 3. (Color online) (a) I-V characteristics for different B at $T = 2.2$ K and (b) 1.0 K. At both T, S-shaped I-V curves with an inflection point are visible just below B_p. The straight lines indicate the voltage at the normal state and other lines are guides for the eye.

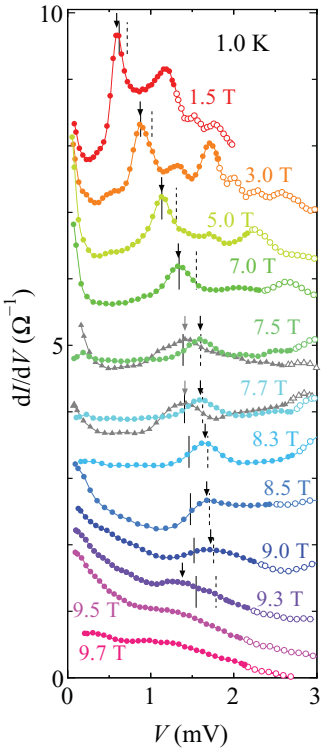

FIG. 4. (Color online) dI/dV vs V at 1.0 K for various B measured with superimposed 10-MHz I_{rf} (circles). For 7.5 and 7.7 T the data measured with $I_{rf} = I_{rf,s}$ and $I_{rf,l}$ are shown with (gray) triangles and circles, respectively. The location of $V_{1/2}^{perp}$ and $V_{1/1}^{para}$ is indicated with short solid and dashed lines, respectively, and other lines are guides for the eye. Arrows mark the peak position. Solid and open symbols correspond to the data for which ΔT <0.01 K and ΔT >0.01 K, respectively. The curves are vertically shifted for clarity.

the results of low-frequency flow noise just above depinning, which exhibits a narrow peak with a sharp rise followed by an almost vertical drop at B_p, it has been revealed[48] that the peak field B_p in $I_c(B)$ marks an order-disorder transition (ODT)[24–27] from the ordered (or weakly disordered) vortex lattice (OP)($B < B_p$) to amorphouslike disordered phase (DP) ($B_p < B < B_c$). B_c at which I_c falls to zero reflects a static "melting" (or depinning) field.

In Figs. 3(a) and 3(b) we show the I-V characteristics for three typical fields at 2.2 K in the thermal regime, where the static melting field B_c is close to the dynamic melting field $B_{c,dyn}$, and at 1.0 K in the quantum regime, where $B_c > B_{c,dyn}$, respectively. A straight line in each figure corresponds to the voltage in the normal state. For both temperatures, peculiar I-V curves with an inflection point are visible in a particular field region just below B_p.

The similar S-shaped I-V curves have been reported in the lower part of PE for $NbSe_2$ crystals, which result from a dynamic coexistence of OP and DP: Most of the sample is in the metastable DP with high I_c at low I, but in the OP with low I_c at high I. In the presence of the current I, the highly pinned DP generated at the sample edges is driven and subsequently annealed into the OP in the bulk.[49] In our a-Mo_xGe_{1-x} films the edge effects are not so important due probably to much smaller sample thickness than the crystals.[50] However, the similarity of the specific I-V curves, as well as flow noise at small velocity (near depinning), just prior to ODT (B_p) observed between the two systems suggests that the picture of the coexistence phase may be also applicable to our films.[49,51]

Figure 4 shows dI/dV vs V taken at 1.0 K for various B with superimposed 10-MHz I_{rf}. Solid and open symbols correspond to the data for which the rise in the local temperature ΔT within the film is below and above 0.01 K, respectively.[35] As schematically illustrated with shading in the inset of Fig. 2(c), we estimate the width of the ML current step by integrating the peak of the dI/dV vs V curves with respect to the flux-flow baseline.[42] Thus obtained value exhibits a broad maximum (ΔI) as a function of I_{rf} and here we focus on the data measured with I_{rf} yielding the maximum ML. As seen from Fig. 4, the peaks in the dI/dV vs V curves (i.e., ML steps) are visible over the broad B up to about 9.3 T.

Assuming a triangular vortex array moving in the direction perpendicular to one side of the triangle(s), we can calculate a value of the voltage ($V_{p/q}^{perp}$) for a given B satisfying the subharmonic resonant condition of $p/q = 1/2$; that is, $V_{1/2}^{perp} = l(p/q)f_{ext}2a_\perp B = lf_{ext}(\sqrt{3}\Phi_0 B/2)^{1/2}$, where l is the distance between the voltage contacts, $2a_\perp$ is the lattice period in the direction of vortex motion [i.e., $a_\perp$ is the row spacing and $(2/\sqrt{3})a_\perp = (2\Phi_0/\sqrt{3}B)^{1/2}$ is the lattice spacing of the triangular lattice], and Φ_0 is the flux quantum [see Fig. 1(b)].[42,44,46] The location of $V_{1/2}^{perp}$ is indicated with a short solid line.

With increasing B, the ML resonance seen in the dI/dV vs V curves changes in the following way: (i) For B =1.5–7 T, the first ML peak voltage V_{peak}, as marked with an arrow, well coincides with the calculation for $V_{1/2}^{perp}$. (ii) As B increases slightly from 7 T, the ML peak becomes broad and I_{rf} dependent, as typically displayed for 7.5 and 7.7 T, where the width of the ML current step exhibits double maximums at different values of I_{rf}[$\equiv I_{rf,s}$ and $I_{rf,l}(\approx 1.7 I_{rf,s})$]. The dI/dV vs V data measured at $I_{rf,s}$ and $I_{rf,l}$ are shown

with (gray) triangles and circles, respectively. It is found that as $I_{\rm rf}$ exceeds around $I_{{\rm rf},s}$, $V_{\rm peak}$ shows a jump from $\approx V_{1/2}^{\rm perp}$ to a value approximately 15% larger than $V_{1/2}^{\rm perp}$. (iii) With further increasing field (B = 8–9 T), $V_{\rm peak}$ takes a value close to $1.15V_{1/2}^{\rm perp}$ for all $I_{\rm rf}$ measured. This resonant voltage is consistent with the condition for the parallel lattice orientation [Fig. 1(a)], which is given by $V_{1/1}^{\rm para} = (2/\sqrt{3})V_{1/2}^{\rm perp}$ and its location is indicated with short dashed lines in Fig. 4. (iv) On approaching B_p(=9.34 T), $V_{\rm peak}$ drops abruptly below $V_{1/2}^{\rm perp}$, simultaneously with ΔI falling to ≈0 (see the next paragraph) and at 9.4 T all evidence for ML disappears.

Summarizing the above results (i)–(iv), the ML data in the high-field region (B = 8–9 T) are better explained by a triangular vortex array moving with the *parallel* orientation, whereas those in lower fields (B = 1.5–7 T) indicate the perpendicular orientation. In the crossover region ($B_{\rm ori}$ = 7.7–8 T) around which the switching of the lattice orientation occurs, the triangular arrays with either orientation may exist depending on the amplitude of $I_{\rm rf}$. At 9.4 T($\approx B_p$) dynamic (quantum) melting of the driven lattice takes place (i.e., $B_{c,\rm dyn} \approx B_p$).

In order to see how the lattice orientation changes with B, we plot in Fig. 2(b) the B dependence of $V_{\rm peak}$ measured at different T ranging from 0.8 to 4.0 K. Over the broad fields the data points fall onto a full curve $V_{1/2}^{\rm perp}(B)$ corresponding to the perpendicular lattice orientation, while for high B, $V_{\rm peak}(B)$ satisfies with the parallel resonant condition given by $V_{1/1}^{\rm para}(B) = (2/\sqrt{3})V_{1/2}^{\rm perp}(B)$, as indicated with a dashed curve. At any T a steplike increase in $V_{\rm peak}(B)$ is visible in the peak regime of $I_c(B)$. This seems to suggest a connection between the lattice rotation and PE. However, when we compare the "peak" behaviors of $V_{\rm peak}(B)$ and $I_c(B)$ more closely, we find that at high T(=2.2, 3.1, and 4.0 K), where $B_{c,\rm dyn}(\approx B_c)$ is higher than B_p, the characteristic field $B_{\rm ori}$[52] at which the lattice rotation occurs nearly coincides with B_p (or ODT), consistent with recent work;[44] by contrast, at lower T(=0.8, 1.0, 1.2 K), where $B_{c,\rm dyn}$ is significantly suppressed from B_c down to B_p, $B_{\rm ori}(\approx 0.8\ B_p)$ is lower than B_p.

Shown in Fig. 2(c) is the field dependence of the (maximum) ML step width ΔI at selected T. After the gradual decrease with field, ΔI exhibits a small dip around $B_{\rm ori}$. This behavior is reasonable, considering that in the particular field region ($\sim B_{\rm ori}$) where the rotation of the lattice orientation occurs, the driven vortex matter shows a trend to be composed of domains with different lattice orientations, which are most likely metastable. This may also explain the jump of $V_{\rm peak}$ from $V_{1/2}^{\rm perp}$ to $V_{1/1}^{\rm para}$ or "bistability" with $I_{\rm rf}$ in addition to the degradation of the ML resonance around $B_{\rm ori}$. As the field exceeds $B_{\rm ori}$, ΔI exhibits a sharp peak followed by a rapid drop to zero at $B_{c,\rm dyn}$. This temporal recovery of ML (the peak in ΔI) observed just above $B_{\rm ori}$ probably results from the growth in the portion of the ordered domains with parallel orientation. The subsequent abrupt drop in ΔI indicates the sudden collapse of the lattice order, evidencing the dynamic melting into a moving liquid. We define the dynamic melting field $B_{c,\rm dyn}$ as a field where $\Delta I(B)$ extrapolates linearly to zero (indicated with a vertical dashed line).[35]

As mentioned above, we find the difference in the relative position of $B_{\rm ori}$ with respect to B_p between the high T and low T regimes. This behavior is better displayed by plotting $V_{\rm peak}/V_{1/2}^{\rm perp}$ ($V_{\rm peak}$ divided by $V_{1/2}^{\rm perp}$) and $I_c/I_c(B_p)$ (I_c divided by the peak value of I_c) at each T(=1.0, 2.2, and 4.0 K) against the reduced field B/B_c, as shown in Figs. 5(a) and 5(b), respectively. Figure 5(b) clearly shows that the peak shape of the $I_c/I_c(B_p)$ vs B/B_c curves is nearly independent of T and hence the reduced peak field $B_p/B_c = 0.84$ (indicated with vertical thick dots), which marks ODT, is also T independent. In Fig. 5(a) horizontal solid ($V_{\rm peak}/V_{1/2}^{\rm perp}$ =1) and dashed ($V_{\rm peak}/V_{1/2}^{\rm perp} = V_{1/1}^{\rm para}/V_{1/2}^{\rm perp} = 1.15$) lines represent the resonant voltages for perpendicular and parallel orientations, respectively. Vertical dashed lines indicate $B_{c,\rm dyn}$ at which $\Delta I \to 0$. In the field region where double maximums in the ML current step with respect to $I_{\rm rf}$ are observed, we plot both values of $V_{\rm peak}/V_{1/2}^{\rm perp}$ measured for $I_{{\rm rf},s}$ and $I_{{\rm rf},l}$. This plot also shows the bistable (or metastable) nature of the lattice orientation in the crossover field regions around $B_{\rm ori}$. It is evident that upon cooling, $B_{\rm ori}/B_c$ (vertical solid lines) shifts to lower fields associated with the decrease in $B_{c,\rm dyn}/B_c$ (vertical dashed lines). We note that the location of B_p deduced from $I_c(B)$ has no direct relation with $B_{\rm ori}$.

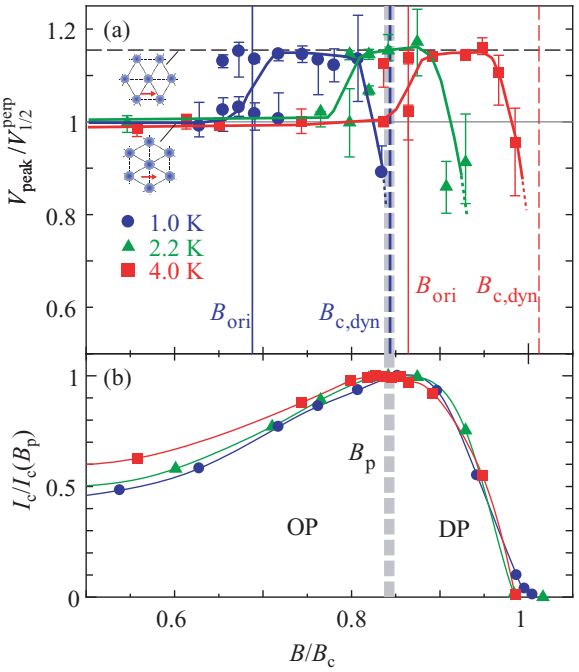

FIG. 5. (Color online) (a) $V_{\rm peak}/V_{1/2}^{\rm perp}$ vs B/B_c at 1.0 (blue circles), 2.2 (green triangles), and 4.0 K (red squares). Horizontal solid and dashed lines indicate $V_{\rm peak}/V_{1/2}^{\rm perp}$ =1 and 1.15, respectively. Vertical solid and dashed lines, respectively, mark $B_{\rm ori}$ and $B_{c,\rm dyn}$; left (blue) and right (red) lines correspond to the fields at 1.0 and 4.0 K, respectively. (Insets) Schematic illustration of moving vortex lattices, where arrows indicate the flow directions. (b) $I_c/I_c(B_p)$ plotted against B/B_c. Symbols correspond to those in (a). Both in (a) and (b), vertical thick dots indicate B_p and other lines are guides for the eye.

The results obtained in this work are summarized in the B-T plane in Fig. 6, where we show $B_{c,\rm dyn}(T)$ (open red circles)[53] and $B_{\rm ori}(T)$ (open green triangles) determined from dynamic measurements of ML, in addition to the equilibrium phase diagram: $B_{c2}(T)$ (open squares), $B_c(T)$ (solid circles), and $B_p(T)$

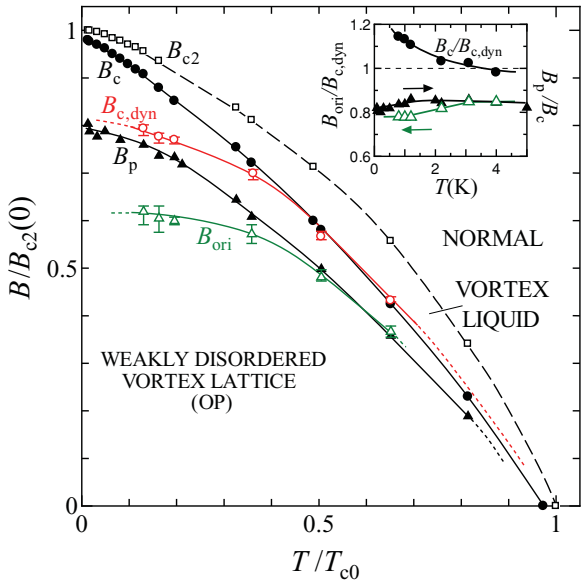

FIG. 6. (Color online) $B_{c,\mathrm{dyn}}$ vs T (open red circles) and B_{ori} vs T (open green triangles) determined from ML measurements. T dependencies of B_{c2} (open squares), B_c (solid circles), and B_p (solid triangles) obtained from static measurements. B and T axes are normalized by B_{c2} at $T = 0$ and T_{c0}, respectively. (Inset) T dependencies of $B_{\mathrm{ori}}(T)/B_{c,\mathrm{dyn}}(T)$ (open green triangles), $B_p(T)/B_c(T)$ (solid triangles), and $B_c(T)/B_{c,\mathrm{dyn}}(T)$ (solid circles). A horizontal dashed line marks unity. Other lines are guides for the eye.

(solid triangles) determined from static measurements.[35] B and T axes are normalized by $B_{c2}(= 12.7\ \mathrm{T})$ at $T = 0$ and T_{c0} at $B = 0$, respectively.[35] Here, we note that the dynamic and static phenomena take place at very different velocities v and that B_{ori} is obtained on the basis of data at a fixed frequency (10 MHz). At high T ($> 0.4T_{c0}$) the shape of the curves of the static characteristic fields, $B_c(T)$ and $B_p(T)$, and the dynamic ones, $B_{c,\mathrm{dyn}}(T)$ and $B_{\mathrm{ori}}(T)$, is similar to each other, whereas at low T($< 0.4T_{c0}$) the T dependencies of $B_{c,\mathrm{dyn}}$ and B_{ori} are much weaker than those of B_c and B_p due probably to strong quantum-fluctuation effects. On the other hand, we notice that over the *whole* T range the shapes of $B_{c,\mathrm{dyn}}(T)$ and $B_{\mathrm{ori}}(T)$ resemble each other, just like the shapes of $B_c(T)$ and $B_p(T)$ do. This is verified by plotting $B_{\mathrm{ori}}(T)/B_{c,\mathrm{dyn}}(T)$, together with $B_p(T)/B_c(T)$, against T. As depicted in the inset of Fig. 6, both ratios (triangles) are nearly constant ($=0.81 \pm 0.03$) or weakly dependent on T over the entire T range, in contrast to $B_c(T)/B_{c,\mathrm{dyn}}(T)$ (circles), which grows at $T \to 0$.

In previous work it has been argued on the basis of data at high T(>2 K) that the switching of the lattice orientation observed around B_p is attributed to proliferation of vortex lattice dislocations being responsible for PE in $I_c(B)$ and ODT.[44] As mentioned above, however, the present data at lower T(<2 K) clearly show that B_{ori} has no direct relation with B_p or static vortex states (ODT). Instead, the lattice rotation is better viewed as a precursor of *dynamic* melting, which is driven either by thermal or quantum fluctuations. The similarity between the shape of the $B_{\mathrm{ori}}(T)$ and $B_{c,\mathrm{dyn}}(T)$ lines and dissimilarity between that of the $B_{\mathrm{ori}}(T)$ and $B_c(T)$ lines are reasonable when we consider that the rotation of the lattice orientation reflects the change in the vortex dynamics and hence it should be related to dynamic melting rather than static melting.

While the experimental data obtained in this work are clear and fundamental, there is no definite idea to explain them comprehensively. We discuss here a qualitative interpretation of the data. In our recent experiment using Corbino-disk a-$\mathrm{Mo}_x\mathrm{Ge}_{1-x}$ films,[54] in which vortices circulate around the center of the disk without crossing the sample edges, it has been suggested that sample edges do not play an important role in the lattice orientation, in contrast to previous expectation.[44] Since the parallel lattice orientation of driven vortex matter has been predicted based on the idea of the minimum power dissipation,[16] several theories and numerical simulations[8,55,56] have proposed the parallel orientation at large velocity. Quite recently, it has been shown numerically using the time-dependent Ginzburg-Landau theory that in thin superconductors with random point pinning, as studied in this work, the lattice orientation of driven vortex matter is parallel in the absence of pinning but perpendicular in the presence of pinning.[45]

Assuming the recent simulation result,[45] we may interpret the field-induced change in the lattice orientation from perpendicular to parallel in terms of decreased dynamic pinning forces that moving vortices feel for B higher than B_{ori}. This leads to a conclusion that the characteristic field where the effective pinning is reduced is expressed as $\approx 0.8B_{c,\mathrm{dyn}}(T)$, which is nearly independent of T. The discussion presented here does not contradict the field dependence of the dynamic pinning force evaluated from I-V characteristics:[47] Judging from a broad peak in $I_c(B)$ at around B_p, the static pinning force just above $B_{\mathrm{ori}}(\approx B_p$ at 4 K) is relatively large, while the *dynamic* pinning force as estimated from the dynamic critical current $I_{c,\mathrm{dyn}}$ remains small or shows a small dip just above B_{ori} and it exhibits a sharp peak at higher B in the vicinity of B_c.[47] Here, $I_{c,\mathrm{dyn}}$ is determined by linear extrapolation of the flux-flow (linear) part of I-V curves to the zero voltage.

To summarize, we report on the lattice orientation of driven vortex matter prior to dynamic melting $B_{c,\mathrm{dyn}}$ in the a-$\mathrm{Mo}_x\mathrm{Ge}_{1-x}$ film based on measurements of the ML resonance. Over the wide temperature range down to near $T = 0$ where quantum melting of driven lattices occurs, we observe a switching of the lattice orientation from perpendicular to parallel under increasing B. Mapping out the dynamic phase diagram in the B-T plane, we find that the shape of the switching field vs T line, $B_{\mathrm{ori}}(T)$, is similar to that of the dynamic melting line $B_{c,\mathrm{dyn}}(T)$, while $B_{c,\mathrm{dyn}}(T)$ at low T is significantly suppressed compared to the static melting line $B_c(T)$ due to quantum effects. The results reveal that the rotation of the lattice orientation occurs as a precursor of dynamic melting instead of static melting. We suggest using recent simulation results that the effective pinning is reduced at $B_{\mathrm{ori}}(T) \approx 0.8B_{c,\mathrm{dyn}}(T)$ prior to dynamic melting irrespective of whether it is driven by thermal or quantum fluctuations.

ACKNOWLEDGMENTS

We thank N. Nakai, X. Hu, and R. Ikeda for useful discussions. This work was supported by a Grant-in-Aid for Scientific Research from the Ministry of Education, Culture, Sports, Science, and Technology of Japan.

[1]S. Bhattacharya, J. P. Stokes, M. J. Higgins, and R. A. Klemm, Phys. Rev. Lett. **59**, 1849 (1987); M. J. Higgins, A. A. Middleton, and S. Bhattacharya, *ibid.* **70**, 3784 (1993).
[2]S. N. Coppersmith and P. B. Littlewood, Phys. Rev. Lett. **57**, 1927 (1986); A. A. Middleton, O. Biham, P. B. Littlewood, and P. Sibani, *ibid.* **68**, 1586 (1992).
[3]E. Barthel, G. Kriza, G. Quirion, P. Wzietek, D. Jerome, J. B. Christensen, M. Jorgensen, and K. Bechgaard, Phys. Rev. Lett. **71**, 2825 (1993).
[4]C. J. Olson, C. Reichhardt, and F. Nori, Phys. Rev. Lett. **81**, 3757 (1998).
[5]W. Henderson, E. Y. Andrei, and M. J. Higgins, Phys. Rev. Lett. **81**, 2352 (1998).
[6]N. Mangan, C. Reichhardt, and C. J. Olson Reichhardt, Phys. Rev. Lett. **100**, 187002 (2008).
[7]D. J. Pine, J. P. Gollub, J. F. Brady, and A. M. Leshansky, Nature (London) **438**, 997 (2005).
[8]L. Balents, M. C. Marchetti, and L. Radzihovsky, Phys. Rev. B **57**, 7705 (1998).
[9]D. López, W. K. Kwok, H. Safar, R. J. Olsson, A. M. Petrean, L. Paulius, and G. W. Crabtree, Phys. Rev. Lett. **82**, 1277 (1999).
[10]G. W. Crabtree, Nature Mat. **2**, 435 (2003).
[11]P. Moretti and M. C. Miguel, Phys. Rev. B **80**, 224513 (2009).
[12]U. Yaron, P. L. Gammel, D. A. Huse, R. N. Kleiman, C. S. Oglesby, E. Bucher, B. Batlogg, D. J. Bishop, K. Mortensen, and K. N. Clausen, Nature (London) **376**, 753 (1995).
[13]A. E. Koshelev and V. M. Vinokur, Phys. Rev. Lett. **73**, 3580 (1994).
[14]J. Van de Vondel, A. V. Silhanek, V. Metlushko, P. Vavassori, B. Ilic, and V. V. Moshchalkov, Phys. Rev. B **79**, 054527 (2009).
[15]Y. Togawa, R. Abiru, K. Iwaya, H. Kitano, and A. Maeda, Phys. Rev. Lett. **85**, 3716 (2000).
[16]A. Schmid and W. Hauger, J. Low Temp. Phys. **11**, 667 (1973).
[17]M. P. A. Fisher, Phys. Rev. Lett. **65**, 923 (1990).
[18]G. Blatter, B. Ivlev, Y. Kagan, M. Theunissen, Y. Volokitin, and P. Kes, Phys. Rev. B **50**, 13013 (1994).
[19]R. Ikeda, Int. J. Mod. Phys. B **10**, 601 (1996); K. Myojin, R. Ikeda, and S. Koikegami, Phys. Rev. B **78**, 014508 (2008).
[20]J. A. Chervenak and J. M. Valles Jr., Phys. Rev. B **54**, R15649 (1996).
[21]M. M. Mola, S. Hill, J. S. Brooks, and J. S. Qualls, Phys. Rev. Lett. **86**, 2130 (2001).
[22]T. Shibauchi, L. Krusin-Elbaum, G. Blatter, and C. H. Mielke, Phys. Rev. B **67**, 064514 (2003).
[23]S. Okuma, Y. Imamoto, and M. Morita, Phys. Rev. Lett. **86**, 3136 (2001); S. Okuma, S. Togo, and M. Morita, *ibid.* **91**, 067001 (2003).
[24]Y. Paltiel, E. Zeldov, Y. N. Myasoedov, H. Shtrikman, S. Bhattacharya, M. J. Higgins, Z. L. Xiao, E. Y. Andrei, P. L. Gammel, and D. J. Bishop, Nature (London) **403**, 398 (2000); M. Marchevsky, M. J. Higgins, and S. Bhattacharya, *ibid.* **409**, 591 (2001); Y. Paltiel *et al.*, Phys. Rev. Lett. **85**, 3712 (2000); Europhys. Lett. **58**, 112 (2002); G. Jung *et al.*, Proc. SPIE. **5112**, 222 (2003); Y. Paltiel *et al.*, Europhys. Lett. **66**, 412 (2004).
[25]C. J. van der Beek, S. Colson, M. V. Indenbom, and M. Konczykowski, Phys. Rev. Lett. **84**, 4196 (2000).
[26]Z. L. Xiao, O. Dogru, E. Y. Andrei, P. Shuk, and M. Greenblatt, Phys. Rev. Lett. **92**, 227004 (2004).
[27]B. Rosenstein and V. Zhuravlev, Phys. Rev. B **76**, 014507 (2007).
[28]P. H. Kes and C. C. Tsuei, Phys. Rev. B **28**, 5126 (1983).
[29]S. Bhattacharya and M. J. Higgins, Phys. Rev. Lett. **70**, 2617 (1993); A. C. Marley, M. J. Higgins, and S. Bhattacharya, *ibid.* **74**, 3029 (1995).
[30]K. Ghosh, S. Ramakrishnan, A. K. Grover, G. I. Menon, G. Chandra, T. V. Chandrasekhar Rao, G. Ravikumar, P. K. Mishra, V. C. Sahni, C. V. Tomy, G. Balakrishnan, D. Mck Paul, and S. Bhattacharya, Phys. Rev. Lett. **76**, 4600 (1996).
[31]A. M. Troyanovski, M. van Hecke, N. Saha, J. Aarts, and P. H. Kes, Phys. Rev. Lett. **89**, 147006 (2002).
[32]S. S. Banerjee, N. G. Patil, S. Saha, S. Ramakrishnan, A. K. Grover, S. Bhattacharya, G. Ravikumar, P. K. Mishra, T. V. Chandrasekhar Rao, V. C. Sahni, M. J. Higgins, E. Yamamoto, Y. Haga, M. Hedo, Y. Inada, and Y. Onuki, Phys. Rev. B **58**, 995 (1998).
[33]Z. L. Xiao, E. Y. Andrei, P. Shuk, and M. Greenblatt, Phys. Rev. Lett. **85**, 3265 (2000).
[34]A. D. Thakur, T. V. Chandrasekhar Rao, S. Uji, T. Terashima, M. J. Higgins, S. Ramakrishnan, and A. K. Grover, J. Phys. Soc. Jpn. **75**, 074718 (2006).
[35]S. Okuma, H. Imaizumi, and N. Kokubo, Phys. Rev. B **80**, 132503 (2009).
[36]A. T. Fiory, Phys. Rev. Lett. **27**, 501 (1971).
[37]P. Martinoli, Phys. Rev. B **17**, 1175 (1978).
[38]L. Van Look, E. Rosseel, M. J. Van Bael, K. Temst, V. V. Moshchalkov, and Y. Bruynseraede, Phys. Rev. B **60**, R6998 (1999).
[39]C. Reichhardt, R. T. Scalettar, G. Zimányi, and N. Grønbech-Jensen, Phys. Rev. B **61**, R11914 (2000).
[40]A. B. Kolton, D. Dominguez, and N. Grønbech-Jensen, Phys. Rev. Lett. **86**, 4112 (2001).
[41]N. Kokubo, R. Besseling, V. M. Vinokur, and P. H. Kes, Phys. Rev. Lett. **88**, 247004 (2002).
[42]N. Kokubo, K. Kadowaki, and K. Takita, Phys. Rev. Lett. **95**, 177005 (2005).
[43]This phenomenon (i.e., the ML resonance) has been observed not only in superconductors with periodic pinning[38,39] but also in those with *random* pinning,[36,40–42] such as amorphous films studied here, where a periodicity can be induced dynamically as a result of the coherent motion[13,15] of a vortex lattice.
[44]N. Kokubo, T. Nishizaki, B. Shinozaki, and P. H. Kes, Physica C **470**, 43 (2010).
[45]N. Nakai, N. Hayashi, and M. Machida, Physica C **469**, 1106 (2009).
[46]N. Kokubo, T. Asada, K. Kadowaki, K. Takita, T. G. Sorop, and P. H. Kes, Phys. Rev. B **75**, 184512 (2007).
[47]S. Okuma, J. Inoue, and N. Kokubo, Phys. Rev. B **76**, 172503 (2007).
[48]S. Okuma, K. Kashiro, Y. Suzuki, and N. Kokubo, Phys. Rev. B **77**, 212505 (2008).
[49]Y. Paltiel, Y. Myasoedov, E. Zeldov, G. Jung, M. L. Rappaport, D. E. Feldman, M. J. Higgins, and S. Bhattacharya, Phys. Rev. B **66**, 060503 (2002).
[50]In the $NbSe_2$ crystals where the thickness d is much larger than the penetration depth λ, vortex lines enter the sample by forming two vortex segments in the opposite sharp corners of the sample edge, which reconnect in the bulk. This results in the formation of a disordered, entangled phase in the sample interior [E. Zeldov, A. I. Larkin, V. B. Geshkenbein, M. Konczykowski, D. Majer, B. Khaykovich, V. M. Vinokur, and H. Shtrikman, Phys. Rev. Lett. **73**, 1428 (1994); M. Marchevsky, M. J. Higgins, and

S. Bhattacharya, *ibid.* **88**, 087002 (2002)]. Such an effective "mechanical entangler" of the vortex lines is supposed to be absent in thin films ($d < \lambda$), where vortices enter the sample as rigid straight lines.[48]

[51]In the coexisting phases the vortex motion should be unstable and accompanied by large velocity fluctuations, which leads to pronounced noise. We have also found that in the particular field region just prior to B_p a cutoff (corner) frequency in the voltage noise spectrum does not reflect a simple time-of-flight dynamics, but requires two characteristic times, both of which increase associated with the increase in low-frequency noise.[48] We consider that observed flow noise at small velocity is dominated by random motion of the metastable DP in the OP.

[52]Here, $B_{\rm ori}$ indicated with a vertical solid line is defined as a field at which $V_{\rm peak}/V_{1/2}^{\rm perp} = 1.08$ [i.e., a midpoint of $V_{1/2}^{\rm perp}(B)$ and $V_{1/1}^{\rm para}(B)$].

[53]In order to show $B_{c,\rm dyn}$ in the limit of zero pinning, we plot the values of $B_{c,\rm dyn}(f_{\rm ext})$ extrapolated to $f_{\rm ext} \to \infty$, instead of $B_{c,\rm dyn}$ taken at finite $f_{\rm ext}$ =10 MHz. However, these two values differ by only a few percent and hence the discussion that follows stays essentially unchanged by using either value.

[54]S. Okuma, Y. Yamazaki, and N. Kokubo, Phys. Rev. B **80**, 220501(R) (2009).

[55]P. Le Doussal and T. Giamarchi, Phys. Rev. B **57**, 11356 (1998).

[56]Q. H. Chen and X. Hu, Phys. Rev. Lett. **90**, 117005 (2003) and private communications.